PROCEEDINGS, 41st Workshop on Geothermal Reservoir Engineering
Stanford University, Stanford, California, February 22-24, 2016
SGP-TR-209

Fractal Modeling of Outcrop Fracture Patterns in Alasehir Geothermal Reservoir Turkey

Emrah GUREL, Yakup B. COSKUNER, Serhat AKIN

Middle East Technical University Petroleum & Natural Gas Engineering Department Ankara, 06531, Turkey

egurel@turkerler.com, coskuner@mines.edu, serhat@metu.edu.tr

Keywords: Box Counting Method, Fractal Modeling

ABSTRACT

Alasehir geothermal area located in Gediz graben is the current high enthalpy geothermal target in Turkey. The geothermal system mainly produces from fractured Paleozoic Menderes metamorphics. In order to characterize the fractured reservoir formations, marble and schist outcrop fracture networks were identified and traced using image analysis software. Primary and secondary fracture histograms were developed and box counting method was used to calculate fractal dimension. It was observed that for both formations average fractal dimensions were close to 1.3 similar to those observed for Kizildere and Germencik geothermal fields. Permeability and porosity estimates were obtained using cubic law and a fractal model. It has been observed that permeability and porosity estimates were in accord with those obtained with well test analysis.

1. INTRODUCTION

Production of electricity by geothermal energy in Turkey has been increasing since 2007. There are several active geothermal fields with total running capacity of 400.23 MWe. (Mertoglu, Simsek, & Basarir, 2015) Alasehir geothermal area located in Gediz graben is the current high enthalpy geothermal target in Turkey. (Turkerler Geothermal Energy, n.d.) Geothermal system of Alaşehir is mainly composed of fractures. Since fractures are heterogeneous and consistent, detailed characterization is needed. Fractal modeling of fractures is important to understand the fluid flow in reservoir. This modeling approach relies on a non-integer number which is called fractal dimension, D_f. (Babadagli, 2001) While the dimension of regular shapes are integer numbers such as a point, an area and a volume has a dimension of 1, 2 and 3 respectively, the dimension of fractal is a non-integer number and it varies. (Wahl, n.d.) There are several methods to calculate D_f; yard stick method, box counting method, variation method, structure function method, root mean square method and r/s analysis method. (Zhong, Zeng, & Xu, 2012) Among these methods box counting method is the most preferred one. (Babadagli, 2001) It is also possible to derive a fractal model for permeability for fractured rocks based on the fractal geometry theory and the cubic law for laminar flow in fractures. (Miao, Yu, Duan, & Fang, 2015)

In order to characterize the fractured Alasehir reservoir formations, marble and schist outcrop fracture networks were identified and traced using an image analysis software (Imagej, n.d.). For the characterization of fracture networks as fractals, Imagej software plugin "Fraclac" is used to estimate "D_f" by using box counting method. Fracture density, porosity and permeability values of outcrops of Alasehir geothermal reservoir rocks were calculated using a method proposed by Miao et al. the. The permeabilities are then compared to those obtained by well test analysis. (Akin, 2015)

2. ALASEHIR GEOTHERMAL RESERVOIR

Alsehir Graben (also known as Gediz Graben) located in the Western Anatolia has east-west trending structures. (Seyitoglu, Cemen, & Tekeli, 2000) The graben aged as Mio-Pliocene was developed under Late Cenozoic north-south extensional tectonics. (Seyitoglu & Scott, 1996) Because there are high density of faults and great number of fault intersection which existed because of tectonic activities, geothermal fluids are able to flow through the high permeable rock. (Faulds, Bouchot, Moeck, & Oguz, 2009) The major feed zones in the upper Paleozoic carbonaceous metamorphics stand at approximately 1150 and 1660 m depth. (Akin, et al., 2015) Both margins of the graben at south and north are dominated by non-marine sediments showing marked lateral and vertical facies variation. (Purvis & Robertson, 2005) The stratigraphy of the region is mainly represented by metamorphic rocks of the Menderes Massif and the synextensional Salihli Granitoid as basement rocks, which are tectonically overlain by Neogene-Quaternary aged sedimentary rocks. (Akin, et al., 2015) Alasehir Graben which contains four sedimentary units developed under an extensional tectonic regime includes possible traps as well as high potential for hydrocarbon generation. (Yilmaz & Gelisli, 2003) The sedimentary units are Alasehir Formation, Kursunlu Formation, Kalatepe Formation and alluvium. In the northern part, the thickness of sedimentary rock section which consists of Miocene and Plio-Quaternary, alluvial–fluvial and lacustrine sedimentary rocks is almost 3 km. (Turk, 2014). A combination of marbles and schists have been identified in some areas as having developed into a fractured geothermal reservoir where production of geothermal fluid at economic rates is possible (Akin et al 2015).

3. PREPARATION OF FRACTURE TRACES

Images were obtained from three different locations at which outcrop of the reservoir rock was observed (Figure 1). To draw a histogram and apply box counting method, the fracture traces were prepared in such a way that several image processing techniques were applied to the outcrop images. The brightness, saturation and color were changed and adjusted for each of these pictures. Moreover, the color images were converted to binary images, which provide opportunity to observe the best possible fracture traces. Figure 2.a and 2.b represent the original outcrop photo and fracture traces drawn after modifying the image via Imagej respectively and

Figure 3.a to 3.j represent the fracture traces. It is important to note that traces presented by Figure 3.a to 3.j do not provide any information about fracture aperture and fracture type.

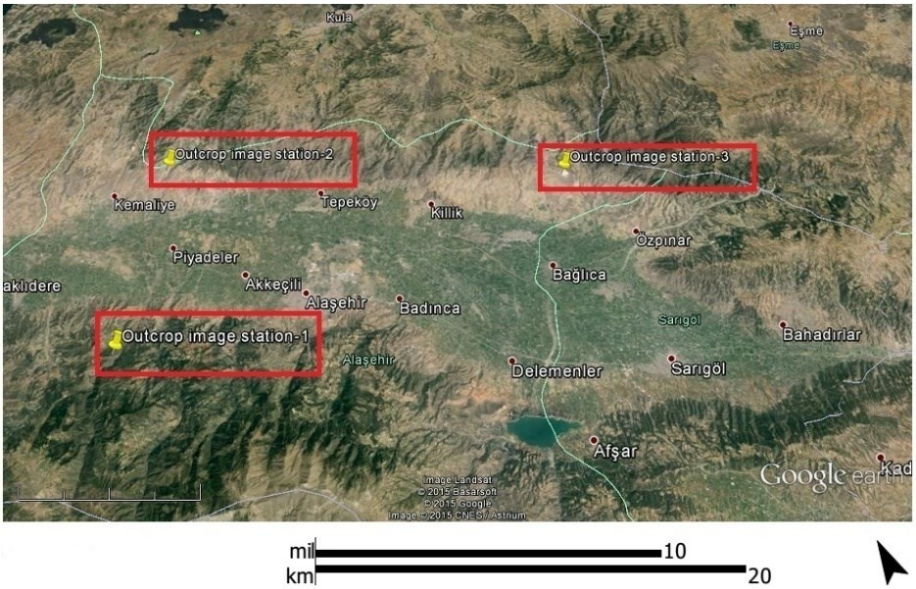

Figure 1: Marble and schist outcrop sampling locations.

a **b**

Figure 2: Comparison of original outcrop image vs. fracture traces

a **b**

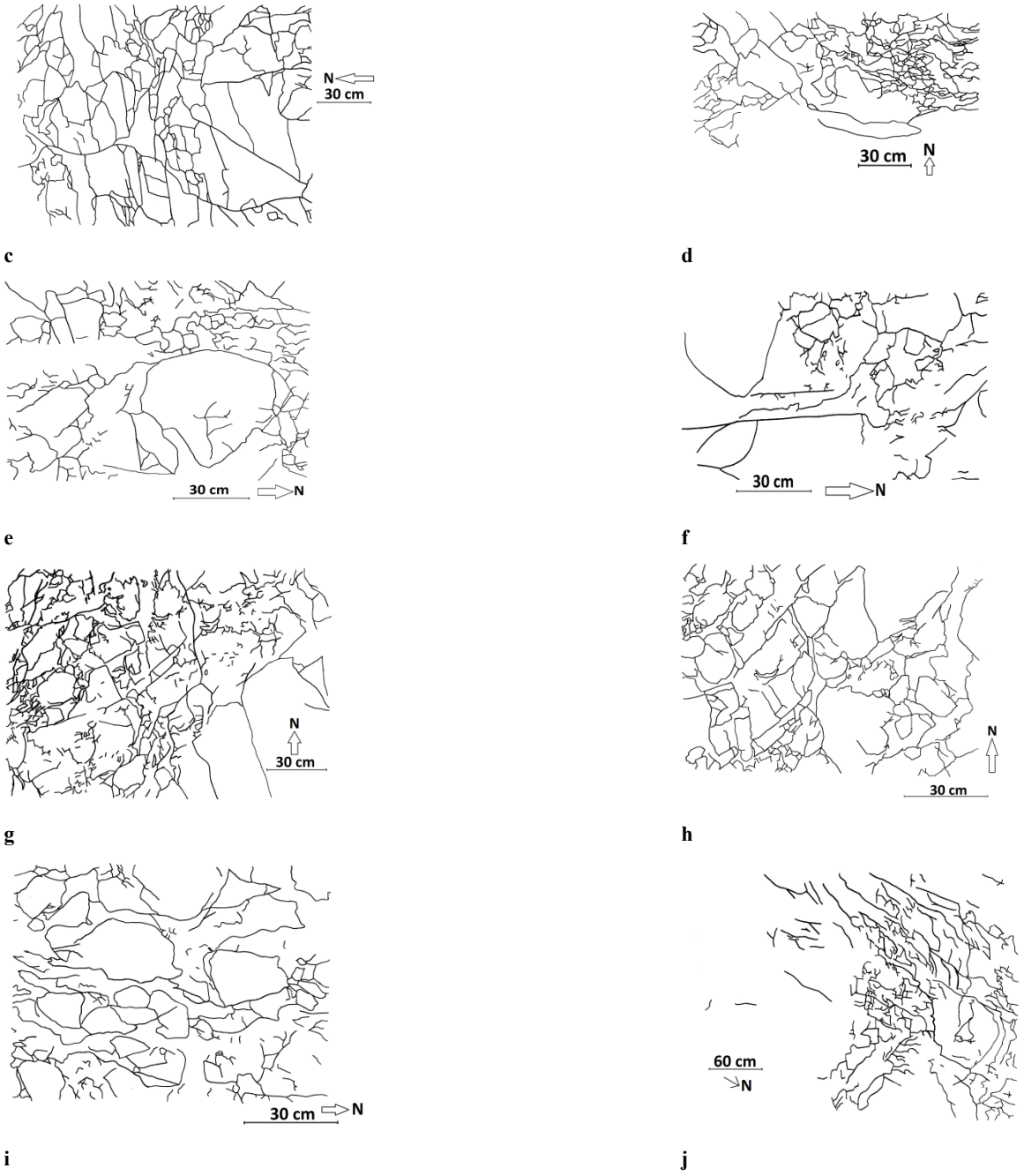

Figure 3: Fracture traces obtained for several outcrop image.

4. RESULTS

4.1 Fractal Dimension

Box counting approach which is a very common used technique to calculate the fractal dimension is used via Fraclac plugin of Imagej software). (Collins, 2007). To achieve this goal, first a series of grids of decreasing size is laid over an image. Then number of fractures present is obtained for each grid size. The boxes have a side length of (d) and there are (N_d) number of boxes. For each of different side lengths (d), different number of boxes is counted. Depending on this information, log(d) vs log(N_d) graph is plotted. Fractal dimension of the image is then calculated by measuring the slope which is typically between 1.0 and 2.0. (Walsh & Watterson, 1993)

For all of the images presented in Figure 3.a to 3.j fractal dimensions were calculated. An illustration for the calculation of D_f of Figure 3.a and the results for the rest are shown in Figure 4 and Table 1 respectively. Average fractal dimension is calculated using box counting method as 1.32 for marble and 1.29 for schist. Similar fractal dimensions are obtained in literature for metamorphic reservoir

rocks of Büyük Menderes Graben (Babadağlı et al., 1997). Fractal dimension for metamorphic rocks at Germencik and Kizildere Geothermal Fields were reported as 1.411 and 1.29 respectively. Fractal dimensions calculated using satellite images for Germencik and Kızıldere fields changed between 1.55 and 1.57 respectively.

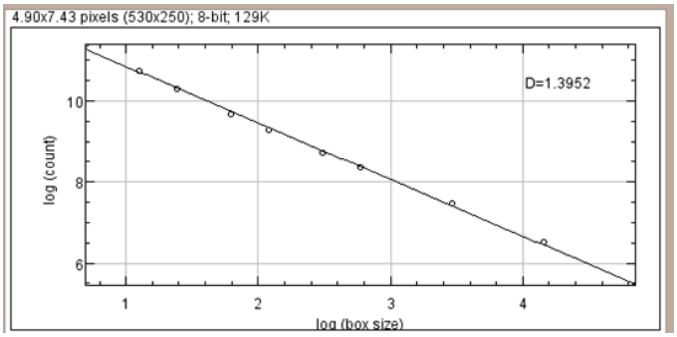

Figure 4: log(d) vs log(N_d) Plot of Figure 3.a

Table 1: Fractal Dimension (D_f) Values of Schist (S) and Marble (M) Outcrops

Sample	Fractal Dimension	Sample	Fractal Dimension	Sample	Fractal Dimension
S-1	1.2670	S-7	1.3381	M-2	1.3065
S-2	1.2024	S-8	1.3023	M-3	1.2756
S-3	1.3152	S-9	1.3204	M-4	1.3121
S-4	1.2730	S-10	1.2743	M-5	1.3359
S-5	1.2825	S-11	1.3420	M-6	1.3739
S-6	1.3141	M-1	1.3081		

4.2 Fracture Density and Width

Utilizing available data as much as possible and generating more realistic fracture networks are two important factors in order to minimize uncertainty. Parameters like fracture density and aperture were studied to further characterize the fracture network. In order to calculate average fracture aperture of each outcrop image, first linear fracture density was measured. The fractures were selected in such a way that 7 random latitudinal and 5 random longitudinal lines were drawn on the original outcrop photos and each fracture that was crossed by a line was used to obtain fracture density in x and y directions for schist and marble images. It was not possible to measure the width of some of these fractures because of the resolution of the photos. As a result, although 350 fractures were identified, only 314 different fractures were measurable. Fracture density values of marble and schist outcrops did not show marked differences, but vertical fracture density (min: 3.97, max: 8.88, average: 5.98) was somewhat lower than the horizontal fracture density (min: 4, max: 14.59, average: 7.56). Thus it can be concluded that there was a directional difference between the vertical and horizontal fracture density values. Using these identified fractures aperture values were obtained. Figure 5 gives histogram of measured apertures, which is lognormal. The lognormal aperture distribution behavior has been observed in several studies (Gale, 1987; Renshaw, 1995), but a Gaussian distribution for the aperture (Hakami and Larsson, 1996; Pyrak-Nolte et al., 1997) is also common. The lognormal behavior is attributed to the high degree of skewness and the long tail of the histograms as in Figure 5.

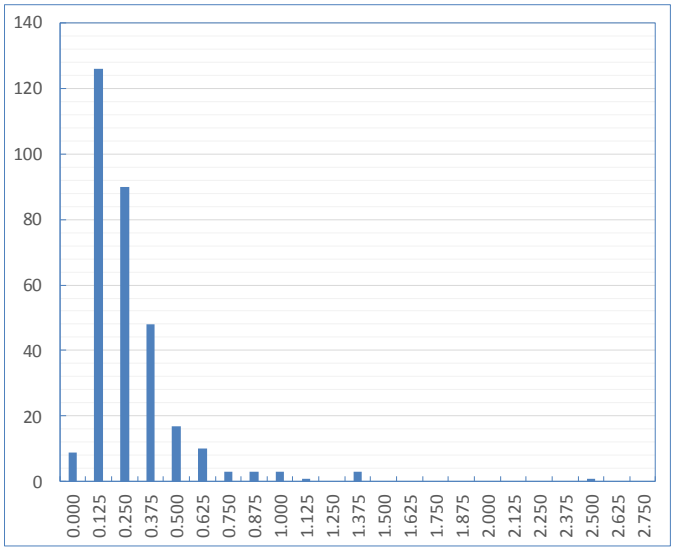

Figure 5: Histogram of Fracture Aperture

4.3 Fracture Porosity and Permeability

A fractal model suggested by Miao et. al (2015) has been used to obtain fracture permeabilities from the calculated fractal dimensions. This model uses a relationship between the permeability and the fractal dimension (D_f) for fracture area, area porosity (or fracture porosity) (Φ), fracture density (D), the maximum fracture length (l_{max}), fracture aperture (a), the fracture azimuth (α) and fracture dip angle (θ). The formula permeability calculation is given in equation 1.

$$K = \frac{\beta^3 * D}{128} * \frac{(1-D_f)}{(4-D_f)} * \frac{l_{max}^3 * (1-\cos^2\alpha * sin^2\theta)}{\left[1-(\phi)^{\frac{1-D_f}{2-D_f}}\right]} \quad (1)$$

In this equation (β) is a coefficient that defines relationship between effective aperture and the fracture length, such that; $a = \beta * l^n$ where (n) is a constant and chosen to be "1" indicating a linear scaling law. Using a (β) value of 0.002 (Jafari & Babadagli, 2011) permeabilities of the fractures were calculated by assuming each outcrop image has a unit area of (A). Then the areal fracture density is calculated by dividing the total length of fractures (l_{total}) which is given by the following equation

$$l_{total} = \int_{l_{min}}^{l_{max}} l.dN(l) = \frac{D_f * l_{max}}{1-D_f}\left[1-\left(\frac{l_{min}}{l_{max}}\right)^{1-D_f}\right] \quad (2)$$

The facture azimuth (α) and facture dip angle (θ) were also measured using the outcrop images via image processing software, Imagej. Average fracture porosity (Φ) is estimated by using equation 3. In this equation d_E is constant having the value of 1 and 2 for two and three dimensions respectively. The permeability calculation workflow starts with measuring maximum fracture length (l_{max}), minimum fracture length (l_{min}), fracture azimuth (α), and the facture dip angle (θ). After calculating the fractal dimension values (D_f), fracture porosity (Φ), total fracture length (l_{total}), unit area (A), fracture density (D) and then the permeability (K) is calculated respectively. The results are shown in Table 2. Akın (2015) studied interference test conducted in Alaşehir reservoir using were four wells. After analyzing test data, storativitiy and transmissibility values were calculated. Storativitiy of each well is reported as $1.34x10^{-6}$, $2.39x10^{-4}$, $5.61x10^{-4}$ and $6.08x10^{-4}$. If compressibility value is assumed as $5.0^{-5}bar^{-1}$, and reservoir thickness is assumed as 1000 meters, porosities are calculated as %0.00268, %4.78, % 11.2 and % 12.2 respectively. These values are in accord with porosity values obtained using fractal analysis. The permeability values obtained from fractal analysis is somewhat larger than those obtained from well test analysis. Cubic law permeabilities are several of order magnitude larger than those found using fractal analysis. Finally, areal fracture density is comparable to aforementioned linear fracture density values.

$$D_f = d_E + \frac{\ln(\phi)}{\ln(l_{max}/l_{min})} \quad (3)$$

Table 2: Fractal Porosity and Permeability

Sample	S-1	S-2	S-3	S-4	S-5	M-1	M-2	M-3	M-4	M-5
Total Fracture Length (L_{total}) (m)	13.62	6.06	9.72	4.85	1.61	7.32	31.81	13.67	6.04	25.93
Unit Area (A) (m^2)	4.62	3.40	2.00	2.09	1.06	0.93	2.22	0.97	0.83	13.13
Fracture Porosity (ϕ)	0.02	0.08	0.06	0.12	0.11	0.07	0.07	0.03	0.05	0.04
Areal Fracture Density (D) (m/m^2)	2.95	1.78	4.85	2.32	1.52	7.83	14.33	14.11	7.30	1.97
Permeability (mD)	76.25	806.40	501.12	119.21	24.70	2536.03	4037.44	523.00	370.77	355.49

6. DISCUSSION

Fractal porosity and permeability data has some sorts of uncertainty. These uncertainties are either due to the physical phenomenon that is responsible for the physical phenomena that is responsible for reservoir development that is inherently random or errors in the predictions and estimations of the real world conditions (Ang and Tang, 1984). The inherent uncertainty is due to the nature of reservoir itself and cannot be decreased. However, it is possible to reduce the estimation and thus modeling uncertainty by use of more accurate models and/or the acquisition of more reliable and widespread data (Ang and Tang, 1984). The error in model prediction can be further subdivided into systematic and random errors. The systematic error is called the bias and it is due to factors that are not taken into account in the estimation that are likely to affect the estimation (Duzgun, 2004). The estimations based on outcrop samples analyzed using image processing algorithms have systematic error, because they do not represent the in situ conditions of the geothermal reservoir. The random error, on the other hand, is due to lack of or limited knowledge. The sampling error that depends on the sample size is an example of such error. The description of the errors can be made by the use of the mean or median and the standard deviation or coefficient of variation.

When systematic errors in porosity values calculated using outcrop images are considered it can be concluded that porosity may be somewhat different than the actual reservoir porosity. Calculated porosity and permeability can be higher than reservoir porosity and permeability due to confining pressure differences. Furthermore, outcrop rocks are exposed to weathering due to wind, rain etc, which may increase porosity. As for the random errors, images obtained from only three outcrop locations are used. The method provided in this study relies on accurate calculation of fractal dimension. The images used to calculate fractal dimension are processed using binarization and thresholding processes that may affect the result. Therefore, fractal porosity and permeability calculations may include some errors and they may not reflect the actual reservoir porosity and permeability.

6. CONCLUSIONS

In order to characterize the fractured Alasehir reservoir formations, marble and schist outcrop fracture networks were identified and traced using an image analysis software. It has been observed that average fractal dimensions calculated using box counting method for both formations was close to 1.3 similar to those observed for Kizildere and Germencik geothermal fields located in western Anatolia. Average fracture density values of marble and schist outcrops did not show marked differences, but vertical fracture density (min: 3.97, max: 8.88, average: 5.98) was somewhat lower than the horizontal fracture density (min: 4, max: 14.59, average: 7.56). Average porosity estimates obtained using a fractal model changed between 0.03 and 0.12 that is find to be in accord with well test derived porosities. It has been observed that permeability estimates obtained from fractal analysis is somewhat larger than those obtained from well test analysis. Finally, it has been found that average schist permeability (362 mD) is somewhat smaller than the average marble permeability (1564 mD)

7. NOMENCLATURE

A = Unit Area (m^2)
α = Fracture Azimuth (°)
β = Proportional Constant
d = Box Side Length
N_d = Number of Boxes
D_f = Fractal Dimension
d_E = Euclid Dimension
D = Fracture Density (m/m^2)
Φ = Average Fracture Porosity
L_{total} = Total Fracture Length (m)
l_{min} = Minimum Fracture Length (m)
K = Permeability (mD)
θ = Fracture Dip Angle (°)

8. REFERENCES

Akin, S. (2015). Design and Analysis of Multi-well Interference Tests. *World Geothermal Congress.* 19 - 24 April, Melbourne, Australia.

Akin, S., Yildirim, N., Yazman, M., Karadag, M., Seckin, C., Tonguc, E., et al. (2015). Coiled Tubing Acid Stimulation of Alaşehir Geothermal Field, Turkey. *World Geothermal Congress.* 19 - 24 April, Melbourne, Australia.

Ang, A.H.S., and Tang, W.H., (1984). Probability Concepts in Engineering Planning and Design, Vol.2. Decision, risk, and reliability. John Wiley and Sons.

Babadagli, T. (2001). Fractal analysis of 2-D fracture networks of geothermal reservoirs in south-western Turkey. *Journal of Volcanology and Geothermal Research*, 83-103.

Collins, T. J. (2007). ImageJ for microscopy. *BioTechniques*, 25-30.

Duzgun, H. S. B., (2004). Reliability-Based Design of Rock Slopes, Ph.D. dissertation, Department of Mining Engineering, Middle East Technical University, Turkey.

Faulds, J. E., Bouchot, V., Moeck, I., and Oguz, K. (2009). Structural Controls on Geothermal Systems in Western Turkey: A Preliminary Report. *Geothermal Research Council Transactions*, 375-381.

Gale, J. E.: Comparison of Coupled Fracture Deformation and Fluid Flow Models with Direct Measurements of Fracture Pore Structure and Stress-flow Properties. The 28th US Symposium on Rock Mechanics (USRMS), (1987).

Hakami, E. and Larsson, E.: Aperture Measurements and Flow Experiments on a Single Natural Fracture, International Journal of Rock Mechanics and Mining Sciences & Geomechanics Abstracts, 33(4), (1996), 395-404.

Imagej. (n.d.). Retrieved 1 9, 2016, from Box Counting: http://imagej.nih.gov/ij/plugins/fraclac/FLHelp/BoxCounting.htm

Jafari, A., and Babadagli, T. (2011). Effective fracture network permeability of geothermal reservoirs. *Geothermics*, 25-38.

Mertoglu, O., Simsek, S., and Basarir, N. (2015). Geothermal Country Update Report of Turkey (2010-2015). *Proceedings World Geothermal Congress 2015.* Melbourne.

Miao, T., Yu, B., Duan, Y., and Fang, Q. (2015). A fractal analysis of permeability for fractured rocks. *International Journal of Heat and Mass Transfer*, 75-80.

Nelson, R. A. (1985). *Geologic analysis of naturally fractured reservoirs.* United States of America: Gulf Professional Publishing.

Pyrak-Nolte, L. J., Montemagno, C. D., and Nolte, D. D.: Volumetric Imaging of Aperture Distributions in Connected Fracture Networks, Geophysical Research Letters, 24(18), (1997), 2343-2346.

Purvis, M., and Robertson, A. (2005, January 3). Sedimentation of the Neogene–Recent Alaşehir (Gediz) continental graben system used to test alternative tectonic models for western (Aegean) Turkey. *Sedimentary Geology*, pp. 373-408.

Renshaw, C. E.: On the Relationship between Mechanical and Hydraulic Apertures in Rough-walled Fractures, Journal of Geophysical Research, 100(B12), (1995).

Seyitoglu, G., and Scott, B. C. (1996). Age of the Alasehir Graben (west Turkey) and Its Tectonic Implications. *Geological Journal*, 1-11.

Seyitoglu, G., Cemen, I., and Tekeli, O. (2000). Extensional Folding in the Alasehir (Gediz) Graben, Western Turkey. *Journal of the Geological Society*, 1097-1100.

Turk, S. (2014). Seismic structure and tectonics of the Alasehir--Gediz Graben, Western Turkey. Oxford, Ohio, United States of America: ProQuest LLC.

Turkerler Geothermal Energy. (n.d.). Retrieved 1 10, 2016, from Turkerler Holding: http://www.turkerler.com/en/energy/geothermal-energy/

Wahl. (n.d.). Retrieved 01 09, 2016, from Fractal Dimenssions: http://www.wahl.org/fe/HTML_version/link/FE4W/c4.htm#_ftnref1

Walsh, J. J., and Watterson, J. (1993). Fractal analysis of fracture patterns using the standard box-counting technique: valid and invalid methodologies. *Journal of Structural Geology*, 1509-1512.

Yilmaz, M., and Gelisli, K. (2003, July). Stratigraphic–structural interpretation and hydrocarbon potential of the Alaşehir Graben, western Turkey. *Petroleum Geoscience*, pp. 277-282.

Zhang, X., and Sanderson, D. J. (1998). Numerical study of critical behaviour of deformation and permeability of fractured rock masses. *Marine and Petroleum Geology*, 535-548.

Zhong, L., Zeng, F., and Xu, G. (2012). Comparison of Fractal Dimension Calculation Methods for Channel Bed Profiles. *Procedia Engineering* (pp. 252-257). Elsevier.